REFEREED PAPER

AN INVESTIGATION INTO THE VISCOSITY OF C-MASSECUITE USING A PIPELINE VISCOMETER

SHAH S[1], LOKHAT D[2] AND PEACOCK SD[3]

[1] *Tongaat Hulett Sugar, Durban, South Africa*
[2] *University of Kwa-Zulu Natal, Durban, South Africa*
[3] *Amalgamated Research LLC, Idaho, USA*

shaista.shah@tongaat.com Lokhat@ukzn.ac.za SPeacock@arifractal.com

Abstract

Most product streams within the sugar process have physical properties that are well defined. However, upon crystallisation, the behaviour of the two-phase product becomes more complex. The physical properties of massecuite affect the design of all equipment and piping in the back-end of a sugar factory, however, the performance of equipment is only as reliable as the data on which the design is based. The massecuite viscosities used within the South African sugar industry were determined over 20 years ago using a rotating viscometer, however, this instrument is believed to be unsuitable for the application due to the heterogeneous nature of massecuite. A pipeline viscometer was thus constructed and experiments carried out to better understand the behaviour of massecuite. This research project aimed to use non-Newtonian theory and data from a pipeline viscometer to determine a correlation for the viscosity of massecuite for varying conditions of temperature, concentration, purity and crystal content taking into account the effects of dextran and crystal size.

Keywords: massecuite, viscosity, pipeline, viscometer, non-Newtonian

Introduction

Massecuite viscosity is a critical physical property in the selection of pumps and the design of equipment in the back end of a sugar mill. The concentration of residual non-sugars and organic salts increases with each boiling, resulting in C-massecuite possessing the lowest purity and highest viscosity. In the absence of a well-established correlation, viscosity data published by Rouillard (1984) as a function of temperature is widely used to estimate C-massecuite viscosity, however, the recommended range is broad and the effect of shear rate is not considered, allowing room for optimisation in the prediction of this parameter.

Accurate prediction of C-massecuite viscosity provides the greatest benefit as this type of massecuite possesses the highest viscosity and is the most difficult to process and thus allows for the greatest capital saving in the back end of a sugar mill.

Extensive research was carried out on the viscosity of massecuite from the 1950s onwards using a rotating viscometer. Whilst the International Commission for Uniform Methods of Sugar Analysis (ICUMSA) accepts the rotational viscometer as the standard technique for measurement of molasses viscosity (Ananta, et al., 1989), this instrument is believed to be unsuitable for massecuite due to the heterogeneous nature of the product (Ananta, *et al.*, 1989). Pipeline

viscometry is favoured for massecuite (Behne, 1964) as no mechanical rotation is involved, limiting the impact of crystal interference or crystal migration on viscosity measurements. Pipeline viscometry uses compressed air as a driving force, which acts evenly upon the massecuite surface, propagating massecuite through the pipeline, and is thus a suitable measuring technique for heterogeneous fluids.

A research project was undertaken to investigate the viscosity of C-massecuite using a pipeline viscometer with the aim to achieve the following:
Design, construct and validate a pipeline viscometer to be used, together with non-Newtonian theory, to determine the flow behaviour index and consistency for C-massecuite as a function of temperature, dissolved solids concentration and crystal content; and
Establish a correlation and guidelines that can be used to assist in the estimation of C-massecuite viscosity.

Newtonian and Non-Newtonian Fluid Behaviour

A fluid's viscosity can be defined as the resistance to flow. The change in fluid viscosity with shear rate allows the fluid behaviour to be classified as Newtonian or non-Newtonian.

Newtonian fluid behaviour

Newtonian fluids are characterised by a constant viscosity μ, independent of the shear rate γ and shear time, and is expressed according to equation 1, where shear stress τ is a measure of the resistive force and shear rate can be defined as the velocity gradient perpendicular to the applied shear. All variables are defined in a nomenclature at the end of the paper.

$$\mu = \frac{\tau}{\gamma} \qquad 1$$

Non-Newtonian fluid behaviour

The complex microstructure associated with heterogeneous, non-Newtonian fluids results in viscosity measurements becoming more complex. Non-Newtonian fluids exhibit a dependence of viscosity on the applied rate of shear and, in some cases, a dependence on time.
Under conditions of increased shear rate, time-independent fluids experiencing a decrease in viscosity (shear thinning) are classified as pseudoplastic whilst fluids required to overcome an initial yield stress thereafter acting as Newtonian fluids are characterised as Bingham plastic, as shown in Figure 1.
Under conditions of constant shear rate over a period of time, time-dependent fluids experiencing a decrease in viscosity are classified as exhibiting thixotropic behaviour.

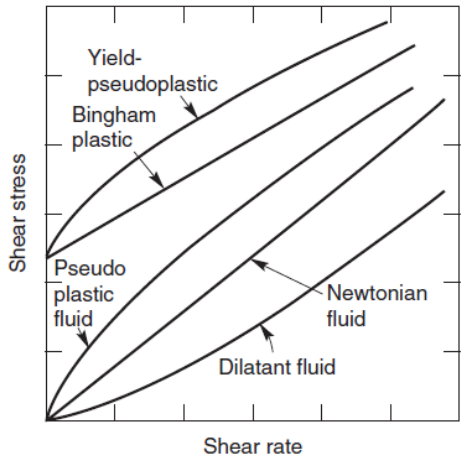

Figure 1. Shear stress-shear rate behaviour for time independent fluid behaviour (Chhabra and Richardson, 2008)

Various authors have classified massecuite as exhibiting either thixotropic, pseudoplastic or Bingham plastic behaviour.

Literature Review

A comprehensive literature review regarding fluid behaviour and the rheology of massecuite was conducted as well as a review of published literature categorised according to the method of viscometry employed.

Power law model

Time independent non-Newtonian fluid behaviour is most commonly expressed by the power law or Ostwald de Waele model (Rouillard, 1985; Chhabra and Richardson, 2008) and is used to characterise massecuite behaviour. The relationship between shear stress and shear rate for a power law fluid is described by equation 2 where K represents consistency and n represents the flow behaviour index. Pseudoplastic fluids are characterised by a flow behaviour index of less than 1, whilst Newtonian fluids can be expressed with a flow behaviour index of 1.

$$\tau = K.\gamma^{n} \quad (2)$$

The apparent viscosity of non-Newtonian fluids can thus be expressed according to equation 3 as a function of consistency, shear rate and flow behaviour index. It can be seen that for Newtonian fluids with a flow behaviour index of 1, consistency is equivalent to viscosity.

$$\mu_{\text{apparent}} = \frac{\tau}{\gamma} = K\gamma^{n-1} \quad (3)$$

Non-Newtonian fluid rheology was used to transform data obtained from experimentation with a pipeline viscometer to calculate the flow behaviour index and consistency for C-massecuite. The equations used are outlined below.

Calculation of shear stress

The shear stress at the wall surface can be expressed according to equation 4 (Chhabra and Richardson, 2008) and applies to both Newtonian and non-Newtonian fluids.

$$\tau_w = \frac{R}{2}\left(\frac{-\Delta P}{L}\right) \quad 4$$

Calculation of shear rate

For an incompressible Newtonian fluid flowing through a pipe, the shear rate can be calculated according to equation 5 (Chhabra and Richardson, 2008).

$$\gamma = \frac{8u}{D} \quad 5$$

The gradient of a ln-ln plot of shear stress τ_w and shear rate γ represents the flow behaviour index, as seen in equation 6.

$$n = \frac{d\ln(\tau_w)}{d\ln\left(\frac{8u}{d_i}\right)} \quad 6$$

For an incompressible non-Newtonian fluid flowing through a pipe, assuming no wall slip, the shear rate at the wall can be calculated according to the Rabinowitsch-Mooney equation 7 (Holland and Bragg, 1995).

$$-\dot{\gamma}_w = \frac{8u}{d_i}\left[\frac{3}{4} + \frac{1}{4}\frac{d\ln\left(\frac{8u}{d_i}\right)}{d\ln(\tau_w)}\right] \quad 7$$

Substitution of equation 6 into 7 simplifies the equation representing non-Newtonian shear rate and can be expressed according to equation 8 (Chhabra and Richardson, 2008).

$$\dot{\gamma}_w = \frac{8u}{d_i}\left[\frac{3n+1}{4n}\right] \quad 8$$

Before being used in the calculation of apparent viscosity, corrections for entrance effects and wall slip were carried out.

Correction for end effects – Calculation of corrected shear stress at the pipe wall

The loss of pressure associated with a developing velocity profile must be correctly accounted for and is commonly referred to as the correction for end effects. The corrected pressure drop for each shear rate can be calculated according to equation 9.

$$\left(-\Delta P_c\right) = \left(-\Delta P\right) - \left(-\Delta P_e\right) \quad 9$$

The corrected pressure drop can then be used to calculate the shear stress at the pipe wall according to equation 10.

$$\tau_w = \frac{R}{2}\left(\frac{-\Delta P_c}{L}\right) \quad 10$$

Correction for wall slip - Calculation of corrected shear rate at the pipe wall

Gases and liquids are collectively classified as fluids and are composed of a number of molecules. These molecules travel an average distance, called the mean free path, before colliding with each other, resulting in a change of path or transfer of energy. As a result of the scale of the apparatus being largely greater than that of the mean free path, the continuum hypothesis can be employed (Holland & Bragg, 1995).

In this hypothesis, the fluid is assumed to act as a continuous medium; the microstructure of the fluid is ignored and the fluid properties represent that of the average prevailing conditions. The continuum hypothesis applies to homogenous and heterogeneous fluids and was applied to massecuite during experimentation with the pipeline viscometer, assuming a uniform distribution of particles up to the pipe wall. The effect of the interaction of crystals at the pipe wall is thereafter accounted for by the associated wall slip (Holland & Bragg, 1995)

An acceleration of particles at the pipe wall is a phenomenon commonly encountered with multi-phase products resulting in a higher system pressure drop. The acceleration is reported to result from a smaller fluid layer at the pipe wall with a lower viscosity resulting in wall slip (Chhabra and Richardson, 2008). The total flow rate of the fluid can be calculated as the sum of the bulk fluid flow and the wall slip flow. For homogeneous fluids, the wall slip velocity u_s is assumed to be zero, simplifying the calculation, however, for a heterogeneous fluid the wall slip velocity is to be accounted for.

Once the wall slip velocity u_s is calculated by graphical determination, the corrected shear rate can be calculated according to equation 11.

$$\dot{\gamma}_{\text{corrected}} = \frac{8u_c}{D} = \frac{8(u - u_s)}{D} \quad 11$$

Application of the power law model and calculation of flow behaviour index and consistency
The power law model can be represented by a straight line on a ln-ln plot of shear stress and shear rate, where the gradient of the straight line represents the flow behaviour index and the intercept represents the consistency. A flow curve is thus developed for each data set based on the corrected shear stress (equation 10) as a function of corrected shear rate (equation 11). It must be noted that the calculation of corrected shear stress and corrected shear rate is an iterative calculation as each correction is dependent on the other.

Substituting equation 8 into 2 yields the following expression for non-Newtonian fluids.

$$\tau = K.\left(\frac{8u}{d_i}\right)^n \left[\frac{3n+1}{4n}\right]^n \quad 12$$

Applying the natural logarithm to both sides of equation 12 yields equation 13, allowing for the development of a straight-line plot of $\ln(\tau_w)$ vs $\ln(\frac{8u}{d_i})$, commonly referred to as a flow curve.

$$\ln(\tau_w) = n\ln\left(\frac{8u}{d_i}\right) + \ln\left(K\left[\frac{3n+1}{4n}\right]^n\right) \quad 13$$

The flow behaviour index and the consistency can be calculated from equation 13 using equations 14 and 15 respectively.

$$n = \text{slope} \quad 14$$

$$K = \frac{e^{\text{intercept}}}{\left[\frac{3n+1}{4n}\right]^n} \quad 15$$

Fluid flow regime and Reynold's number

For a non-Newtonian fluid, however, the Reynold's number becomes a function of the apparent viscosity and can be calculated from a generalised correlation as shown by equation 16.

$$\mathrm{Re}' = \frac{\rho d_i u}{\mu_{apparent}} \quad 16$$

Substituting equations 3 and 5 into 16 yields the correlation for the generalised Reynold's number. The generalised Reynold's number was calculated according to equation 17 to confirm a laminar flow regime under experimental conditions.

$$\mathrm{Re}' = \frac{\rho u^{2-n} d_i^n}{8^{n-1} K} \quad 17$$

Observation of time-dependent behaviour of massecuite

As referenced by Ness (1983), work carried out by Done illustrated thixotropic behaviour of massecuite characterised by time-dependent shear thinning. However, with experimentation using a Brookfield Synchro-Lectric rotating viscometer, Behne (1964) found that the observed time-dependent shear-thinning behaviour was attributed to the displacement of crystals during rotation of the spindle, resulting in the spindle rotating in a pool of molasses.

The instability of crystal suspensions can also contribute toward the observation of time-dependent behaviour, where sedimentation of crystals results in a reduction in the recorded shear stress. Massecuite containing crystals smaller than 0.1 mm with a crystal content less than 30 % is reported to create a stable suspension that enables the use of a rotational viscometer (Ananta, *et al.*, 1989). However, whilst C-massecuite, with typical crystal sizes of 0.12 mm and a crystal content of 28 %, allows for a stable suspension of crystals, the void created by the rotating spindle is still problematic.

Observation of time independent behaviour of massecuite

Massecuite is accepted to exhibit time-independent pseudoplastic behaviour, characterised by a reduction in viscosity with an increasing rate of shear, confirmed by Behne (1964), Ness (1980), Ness (1983), Rouillard (1985), Broadfoot and Miller (1990), Echeverri, *et al*. (2005) and Rein (2007).

As referenced by Awang and White (1976), and Ness (1983), literature from Done, Znamenskii and Popov and Troino reported massecuite to exhibit Bingham plastic behaviour. Bingham plastic fluids are characterised as having an initial yield stress that prevents the fluid from flowing unless overcome by an external force thereafter followed by Newtonian behaviour, as shown in Figure 1. However, Awang and White (1976) referenced work by Adkins (1951), Silina (1953) and Kot, *et al.* (1968) who conducted more detailed experimental work confirming that massecuite will flow under all conditions of shear stress.

Adkins (1951) conducted tests with a Searle viscometer designed by the Bureau of Sugar Experiment Stations in Brisbane. Massecuite samples with crystal contents between 20 % and 40 % were tested by Adkins (1951) and confirmed to exhibit pseudoplastic behaviour, as shown in Figure 2. Adkins noted that observed Bingham plastic behaviour can be attributed to extrapolation of results from tests carried out at a higher shear stress and shear rate, where the shear stress-shear rate relationship is largely linear. However, upon closer examination, massecuite is found to exhibit pseudoplastic behaviour at a lower shear stress whilst overcoming an inherent resistance before achieving a linear flow curve typical of Newtonian behaviour.

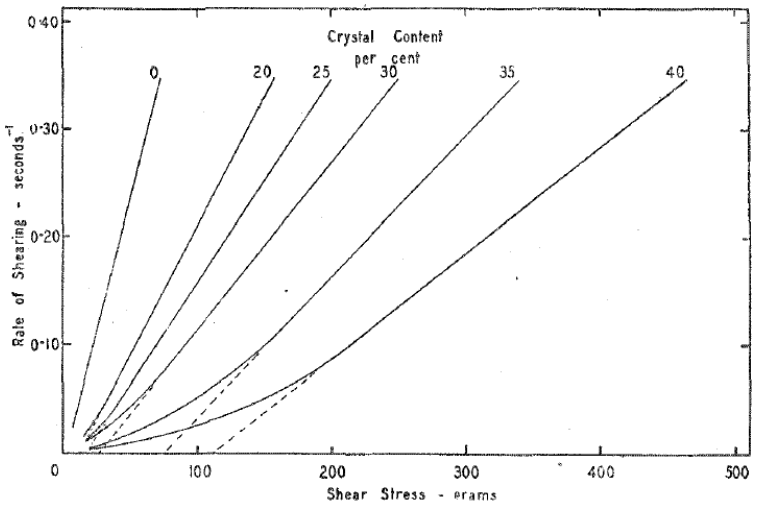

Figure 2. Flow curve developed by Adkins (1951) of shear rate (s^{-1}) vs. shear stress (grams)

Massecuite flow behaviour index, n

The flow behaviour index is indicative of the degree of non-Newtonian behaviour where a value of 1 is indicative of Newtonian behaviour. Studies by Awang and White (1976) showed the flow behaviour index for massecuite to lie between 0.8 - 0.9 and was confirmed by Barker (2008). However, Broadfoot and Miller (1990) reported flow behaviour indices closer to 1. A comparison of published data for the flow behaviour index of massecuite as summarised by Awang and White (1976) is shown in Table 1.

Table 1. Flow behaviour indices for massecuite by Awang and White (1976)

Source	Number of experiments	Temperature	Crystal content	Crystal size range	Shear rate	Range of n	
		^{0}C		mm	s-1		
Done, 1950	12	40-50	15-45	0.3-0.8	0.1-1.5	0.85	+/- 0.04
Adkins, 1951	5	room	20-40	N/A	0.1-4	0.6 - 0.9	
Nicklin, 1958	36	room	5-30	0.3-2.1	0.1-4	0.9	+/- 0.05
Kot et al, 1968	-	20-30	15-50	0.2-0.4	1-30	0.8 - 1	
Awang and White, 1976	22	30-60	15-30	0.3	2-100	0.92	+/- 0.07

Awang and White (1976) proposed that the value of n was independent of crystal content and crystal size but may be dependent on the range of shear rate. At higher shear rates, massecuite behaviour is reported to approach Newtonian behaviour (Ness, 1983) and is reflected in the higher flow behaviour indices calculated by Kot *et al* (1968) and Awang and White (1976).

Massecuite consistency, K

The viscosity of massecuite was historically expressed as an absolute viscosity. The use of the Power Law model to express massecuite consistency correlations can be traced to Durgueil (1987) and Metzler (1996). Durgueil (1987) proposed an Arrhenius-type equation to express consistency as a function of temperature, crystal content, pol and total solids. Metzler (1996) reported an empirical correlation for the consistency of massecuite expressed as a function of molasses consistency and the volume fraction of crystals.

Of the correlations developed using the rotating viscometer, the correlations most widely used are that of Broadfoot, *et al*. (1998) who proposed an equation for molasses consistency and modified the co-efficient of the massecuite consistency correlation by Metzler (1996), and Awang and White (1976) to achieve a better fit.

Factors affecting massecuite viscosity

The viscosity of a crystal suspensions is often expressed as a function of the properties of the suspending mother liquor and/or of the crystals in suspension (Kelly, 1958). The viscosity of massecuite is no different and was historically expressed either as an absolute viscosity or as a function of molasses (molasses dry substance, temperature and purity) and sugar crystals in suspension (crystal content, shape and crystal size distribution). This method of expressing massecuite viscosity was convenient as previous studies included experimentation with massecuite samples prepared in a laboratory by mixing known quantities of molasses and sugar crystals. As a result, the crystal size distribution of dried sugar could be easily determined using a vibrating sieve before addition to molasses and the properties of molasses could be determined directly before mixing.

Experimentation was carried out with massecuite samples directly from Maidstone mill and the dependence of massecuite viscosity on massecuite temperature, massecuite dry substance and crystal content was investigated.

Molasses viscosity

The viscosity of massecuite was found to be highly dependent on the viscosity of the molasses in it as shown by Silina (1953), Kelly (1958), Artyukhov and Garyazha (1970), Awang and White (1976), Metzler (1996), Broadfoot, *et al*. (1998), and Bruhns (2004). In addition, molasses viscosity shows a great dependence on molasses temperature and dry substance, as shown by Rouillard and Koenig (1980) and Broadfoot (1984), as well as impurities present. The risk associated with expressing massecuite viscosity as a function of molasses viscosity is highlighted by Kelly (1958) in that deviations of molasses viscosity from predicted behaviour are transferred to massecuite viscosity predictions.

Awang and White (1976) indicated that work by Nicklin (1958), Done (1950) and Kot *et al* (1968) showed that massecuite and molasses exhibit the same degree of pseudoplasticity. Massecuite viscosity is dependent on the main factors affecting molasses viscosity, namely molasses temperature and molasses dry substance (Rouillard and Koenig, 1980; Broadfoot, 1984), as well as impurities present.

Temperature

As massecuite temperature increases, the vibration of molecules increases and facilitates flow with less friction. A strong dependence of massecuite viscosity on temperature was reported either directly by Rouillard (1984), Durgueil (1987) and Rein (2007) or indirectly as a function of molasses viscosity by Rouillard and Koenig (1980) and Broadfoot (1984).

Rein (2007) noted a strong dependence of massecuite consistency on temperature referencing the viscosity chart developed by Rouillard (1984) as shown in Figure 3, noting a two-fold change in massecuite viscosity with a change in temperature of 10 ^{0}C. Rein (2007) referenced the work of Keast and Sichter (1984) and Barker (1998) as supporting this observation.

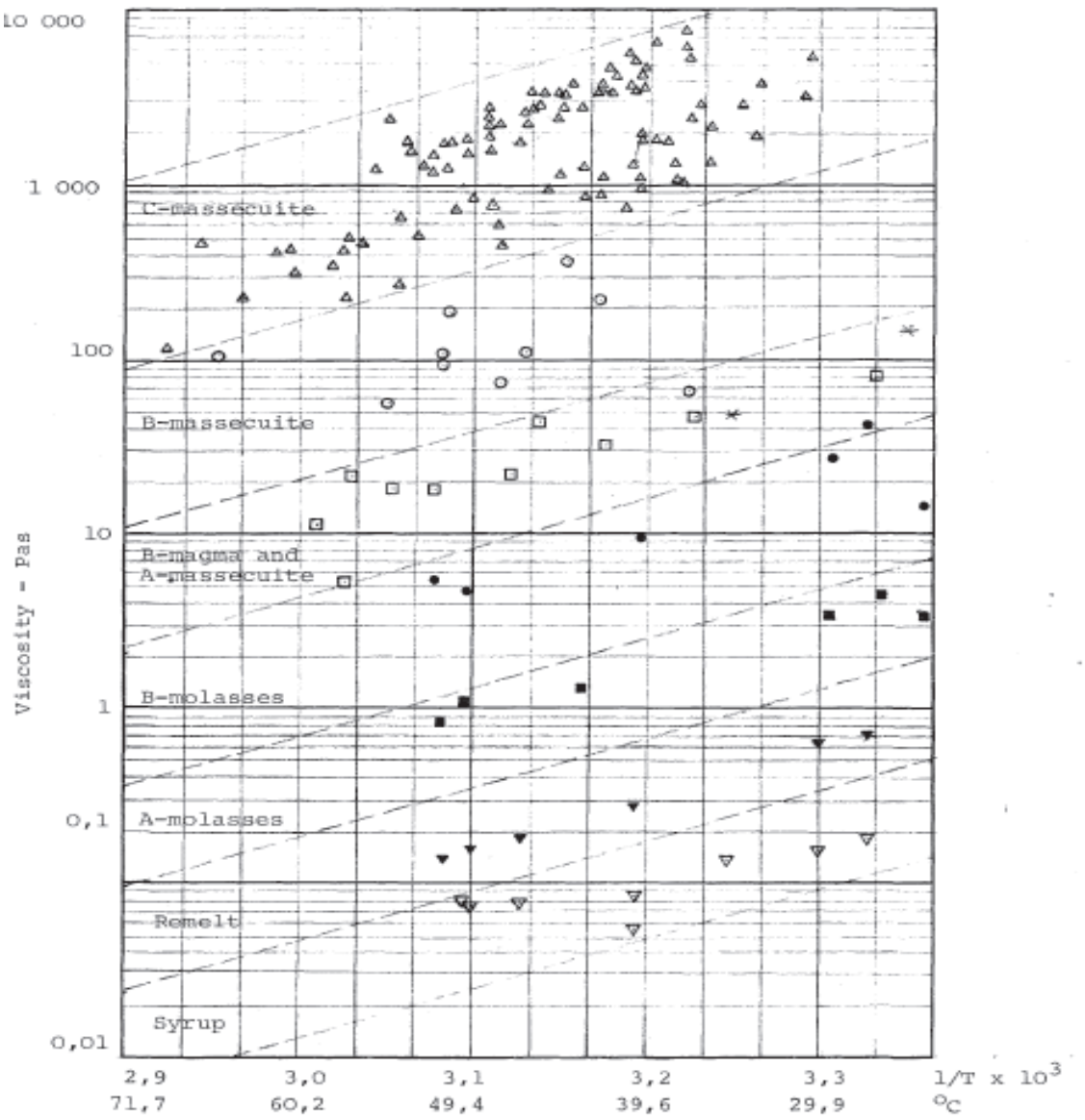

Figure 3. Massecuite viscosity as a function of temperature (Rouillard, 1984)

Broadfoot (1984) and Durgueil (1987) reported a similar change in massecuite viscosity but with a temperature difference of 7 ^{0}C and 9 ^{0}C, respectively. Following a review of the literature, Rein (2007) proposed the use of Figure 4 to determine the range of massecuite and molasses viscosities assuming a two-fold change in viscosity with a temperature difference of 9 ^{0}C.

Viscosity charts as shown in Figure 3 and 4 are commonly used to represent the viscosity-temperature relationship for liquids (Seeton, 2006). The viscosity-temperature relationship presented on a log-log plot is often found to be linear (Perry, 1950) until a critical viscosity is reached, breaking down thereafter to an exponential relationship.

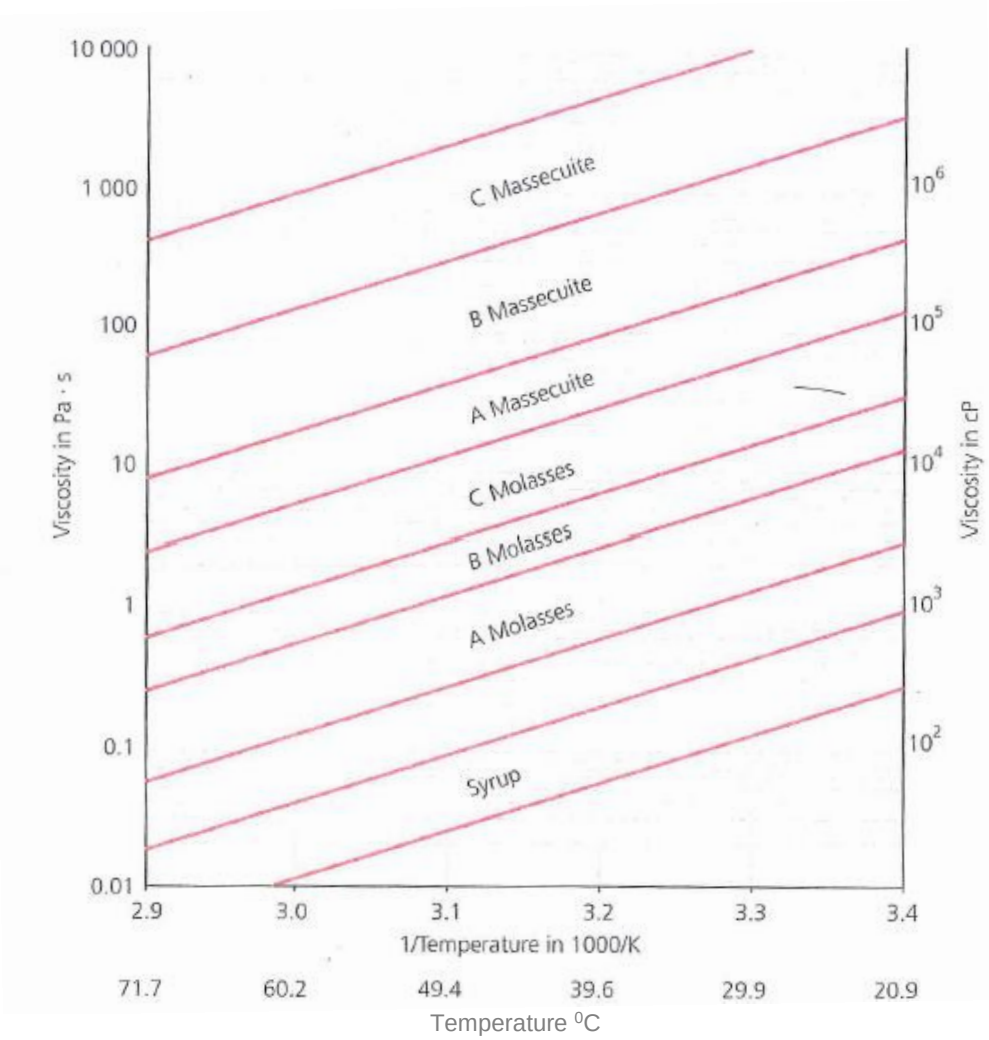

Figure 4. Massecuite viscosity as a function of temperature (Rein, 2007)

Dry substance

The dry substance, or solids concentration, increases as the volume fraction of water decreases. The mobility of suspended crystals is reduced and there is a greater resistance to flow. Dry substance can be calculated according to a correlation proposed by Love (2002) as shown in equation 18.

$$DS = Brix\left(1 - 0.00066\left[Brix - Pol\right]\right) \quad 18$$

Molasses and massecuite viscosity correlations were reported to be strongly dependent on molasses dry substance and were reported either directly (Ness, 1980) or indirectly as a function of molasses viscosity as shown by Silina (1953), Kelly (1958), Artyukhov and Garyazha (1970), Awang and White (1976), Rouillard and Koenig (1980), Broadfoot (1984), Metzler (1996), Broadfoot, *et al*. (1998), and Bruhns (2004).

Crystal content or volume fraction of crystals

The viscosity of massecuite is highly dependent on the crystal content as a mass fraction of crystals (Ness, 1980) or as a volume fraction of crystals, as shown by Silina (1953), Kelly (1958),

Artyukhov and Garyazha (1970), Awang and White (1976), Rouillard and Koenig (1980), Broadfoot (1984), Metzler (1996), Broadfoot, *et al*. (1998), and Bruhns (2004).

The friction caused by particle-fluid and particle-particle interaction in heterogeneous fluids results in a higher resistance to flow. This phenomenon is more pronounced as the quantity of crystals (either mass fraction or volume fraction) increases, and is associated with an increase in viscosity.

Crystal shape

Crystals can be classified as rectangular, D-shaped, elongated or irregular. A rectangular crystal shape is desired, however, the inclusion of impurities on the crystal surface can inhibit growth on a surface, resulting in elongated crystals. Partial dissolution or crystal breakage may result in irregular crystal shapes.

The shape of suspended particles impacts the viscosity of the suspension as the particle orientation during flow and volume required for rotation changes as the particle shape changes (Mueller, *et al.,* 2011). It is thus understandable that the viscosity of massecuite was reported to be dependent on crystal shape, as reported by Kelly (1958), Awang and White (1976), Metzler (1996) and Rouillard and Koenig (1980).

Crystal size distribution

Awang and White (1976) showed a dependence of massecuite viscosity on crystal size distribution reinforced by Rouillard and Koenig (1980) and later confirmed by Metzler (1996) and Broadfoot, *et al*. (1998). Rouillard and Koenig (1980) reported a reduction in massecuite viscosity for a mixture of crystal sizes for the same crystal content.

Impurities

Rouillard and Koenig (1980) identified possible sources of error in massecuite viscosity prediction due to the presence of colloids, dextran or suspended matter present in molasses, believed to increase the viscosity of massecuite. Rouillard (1983) reported that the presence of gums increases massecuite viscosity but noted that insoluble matter and colloids have no measurable effect on the viscosity of factory products. Dextran is believed to increase molasses and thus massecuite viscosity significantly (Rein, 2007). The dextran content on massecuite was measured but used for information purposes only.

Air

The aeration of molasses was reported to inflate molasses viscosity (Rein, 2007) and thus implies an increase in massecuite viscosity. Kelly and McAntee (1942) proposed a method for degassing of molasses samples by exposure to vacuum, prior to mixing with sugar crystals to produce massecuite samples. Massecuite samples were taken directly from the plant at a temperature of approximately 60 ^{0}C and cooled overnight to 45 ^{0}C in a sealed massecuite tank, with the vent valve closed. The cooling effect resulted in the creation of a vacuum and upon opening the vent valve the following day, allowed for de-aeration of each sample. No other exposure to a controlled vacuum environment was possible due to the large quantity of samples utilised.

Shear rate

The non-Newtonian nature of massecuite implies an inherent dependence on shear rate. At higher shear rates, massecuite behaviour was reported to approach Newtonian behaviour (Ness, 1983) and is reflected in the higher flow behaviour indices calculated by Kot, *et al*. (1968) and Awang and White (1976), as shown in Table 1. It is important that experimentation be carried out within the industrially-relevant range of shear rates. Broadfoot and Miller (1990) reported a range of 0.1

– $10s^{-1}$ as being a practical range of shear rates encountered in operation, however, a range of 0.01-$4s^{-1}$ is to be investigated in order to include massecuite flow under gravity and pumped flow.

Pipeline viscometry and associated correlations

Research on the use of the pipeline viscometer for massecuite viscosity measurement has been propagated by the Australian Sugar Industry with very little research done in South Africa. Behne (1964) undertook an investigation into the viscosity of C-massecuite following the inclusion of continuous centrifugals in the Australian sugar industry. Viscosity measurements were carried out using a Brookfield Synchro-Lectric Rotating viscometer and with pipelines of three different lengths, each with low length-to-diameter ratios. Behne (1964) found that the Brookfield viscometer indicated thixotropic behaviour, a time-dependent shear-thinning behaviour that was attributed to the displacement of crystals resulting in the spindle rotating in a pool of molasses. Even as early as 1964, Behne (1964) laid the foundation for the move away from the Brookfield viscometer for massecuite viscosity measurement toward a pipe flow measurement for massecuite viscosity.

The design of the pipeline viscometer is based on the principle that when a fluid flows in the pipeline, a pressure drop results as there is an inherent resistance to flow. Compressed air is used as a driving force, pushing the massecuite through the pipe and the pressure drop is measured using pressure indicators.

Ness, 1980

The work carried out by Ness (1980) took cognisance of the learnings from Adkins (1951), Behne (1964), and Awang and White (1976) and laid the foundations for the practical use of pipeline viscometry for the measurement of massecuite viscosity. A pipeline viscometer was built at the University of Queensland and used to develop a correlation for massecuite viscosity as a function of crystal content and molasses dry solids at a constant temperature of 50 ^{0}C as shown by equation 19.

$$\ln \mu_{\text{massecuite}} = -9.74 + 0.078CC + 0.162DS_{\text{mol}} \qquad 19$$

Ness, 1983

Ness (1983) carried out a comparative study where the viscosity of massecuite was measured using both a pipeline viscometer and a Brookfield RVT rotational viscometer. Both studies showed massecuite to exhibit pseudoplastic behaviour with a good fit to the power law model. Results from the pipeline viscometer illustrated that the flow behaviour index was the same irrespective of the tube dimensions, with changes noted only with the consistency.

Broadfoot and Miller, 1990

An extensive study on the rheology of molasses and massecuite was carried out by Broadfoot and Miller (1990) using a pipeline viscometer. A combination crystalliser-pipeline viscometer was used with water-jacketed tubes with different length-to-diameter ratios.

Massecuite samples were prepared by mixing raw sugar and final molasses to produce a massecuite with a 30 % crystal content by weight. Results from the pipeline viscometer were corrected for end effects and the flow behaviour indices were found to range from 0.86 – 1. Comparison of results with the rotating viscometer was reported to be difficult due to the difference in the range of shear rates, however, it was found that a length to diameter ratio of greater than 35 was required in order for entrance effects to be negligible, i.e. less than 10 % of the total pressure drop.

Bruhns, 2004

Bruhns (2004) carried out an investigation into the viscosity of massecuite using a double tube pipeline viscometer, as shown in Figure 5. Corrections for end effects and wall slip were carried out and the relative viscosity of massecuite was expressed as a function of only molasses viscosity and volume fraction of crystals, as shown in equation 20, where ϕ_{max} = 0.62.

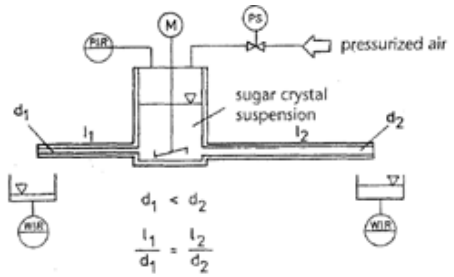

Figure 5. Double tube pipeline viscometer used by Bruhns (2004)

$$\frac{\mu_{massecuite}}{\mu_{molasses}} = 1 + 2.8\left(\frac{\phi}{\phi_m - \phi}\right)^{\frac{4}{3}} \quad 20$$

Barker, 2008

Barker (2008) carried out a comparative study and investigation into the suitability of the pipeline viscometer for measurement of C-massecuite viscosity, comparing results with a Brookfield rotating viscometer. Samples of C-massecuite were prepared by mixing C-sugar and C-molasses and were tested at 55 ^{0}C and 65 ^{0}C. The pipeline viscometer tests were conducted with a single pipe with a length-to-diameter ratio of 40. End effects were ignored as they were reported to be small at low flow rates and for length to diameter ratios of 10-20 (Ness, 1980).

Barker (2008) reported that higher consistencies were measured with the pipeline viscometer than with the rotating viscometer, an observation opposite to that reported by Ness (1980). A linear relationship with crystal content was observed for each sample, however, the slope of each linear relationship was found to be different.

Regarding experimental work with final molasses, the flow behaviour indices were reported to be comparable between the two methods with relatively good agreement.

Pipeline Viscometer and Experimental Considerations

The pipeline viscometer comprises of a pipe attached to the base of a tank, as shown in Figure 6. The viscometer used for this study, classified as a pressure vessel, was designed according to the PD 5500 design code, fabricated according to the pressure vessel regulations as outlined in the Occupational Health and Safety Act of 1993 and approved by an Approved Inspection Authority. The pipeline viscometer is suitable for both Newtonian and non-Newtonian fluids, however, it is not suitable for viscosity measurement of fluids exhibiting time-dependent behaviour or for low-viscosity fluids.

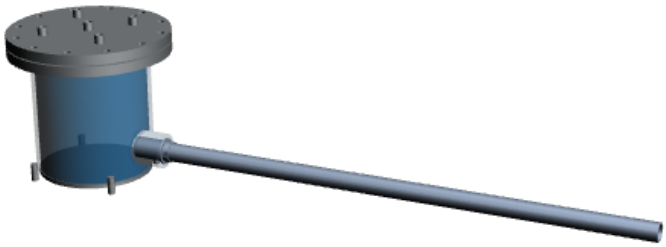

Figure 6. 3D illustration of the pipeline viscometer

The pipeline viscometer was submerged in a temperature controlled water bath, with only a small section of the pipeline exposed to facilitate collection of samples. The water temperature was controlled by an electric heater, as shown in Figure 7. Two submersible pumps assisted with circulation and prevented localised heating. Compressed air was used to create the pressure driving force. The differential pressure was measured using an absolute pressure transmitter and massecuite temperature was recorded. A stirrer was not considered necessary due to the high viscosity associated with C-massecuite, allowing the effects of crystal settling to be ignored.

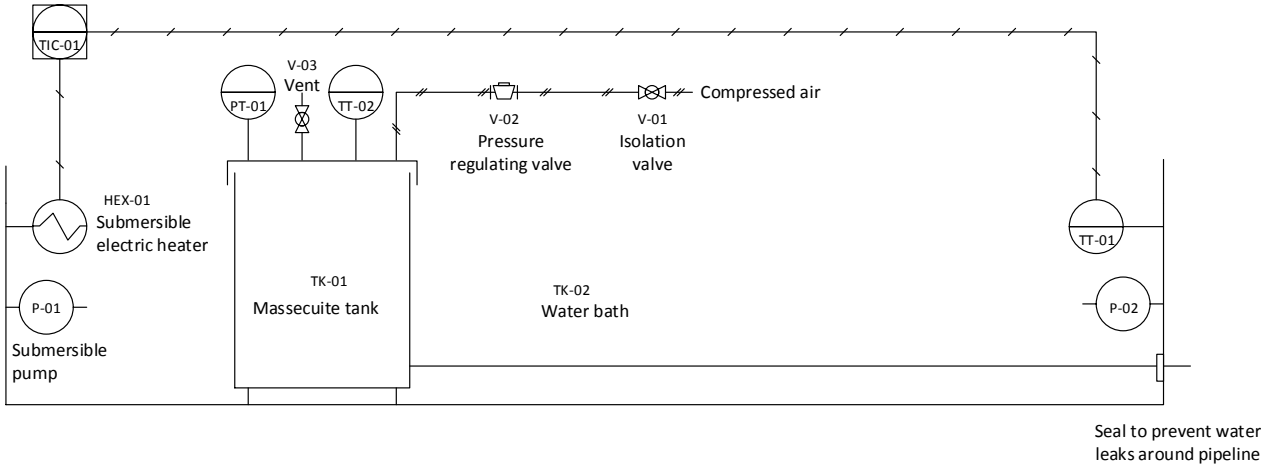

Figure 7. Piping and instrumentation diagram of the experimental apparatus

Shear stress and shear rate was calculated from the massecuite velocity and pressure driving force allowing for the determination of the flow behaviour index and consistency. The experimental apparatus is shown in Figure 8.

Figure 8. Pipeline viscometer in the waterbath

Pipeline design

The massecuite tank was designed to accommodate a working volume of 10 L above the pipe outlet and withstand a maximum pressure of 600 kPa.g. The massecuite tank height was specified as 300 mm with a diameter of 250 mm nominal bore. The viscometer and pipelines are shown in Figure 9. Five pipelines were required with varying internal diameters (ID) and length-to-diameter ratios (LD), as summarised in Table 2.

Figure 9. Pipeline viscometer after fabrication with pipelines

Table 2. Summary of dimensions for pipelines

Tube	Diameter (NB)	ID (m)	Length (m)	LD ratio	Purpose
T1	15	0.01576	0.6	48	Entrance effects
T2	15	0.01576	1	80	Entrance effects
T3	15	0.01576	1.4	112	Routine experiments/ Entrance effects/ Wall slip
T4	25	0.02664	1.4	53	Wall slip
T5	32	0.03508	1.4	40	Wall slip

Range of shear rates for massecuite

Correlations for massecuite viscosity are applicable over a specified range of shear rates. Broadfoot and Miller (1990) recommended an applicable range of shear rate of 0.1 – 10 s^{-1}. However, in order to include massecuite flow under gravity, a narrower industrially-relevant range of shear rates was explored between 0.01 – 4 s^{-1}.

Development of flow curve

The flow curve was generated by plotting the shear stress vs shear rate curve, corrected for end effects and wall slip. The slope of the flow curve represents the flow behaviour index and the intercept represents ln(K), the natural logarithm of the massecuite consistency.

Validation

In order to validate the results from the pipeline viscometer, the viscometer was used to test a fluid of known viscosity, preferably a fluid exhibiting pseudoplastic behaviour similar to massecuite. Carboxymethyl Cellulose (CMC) was originally selected as the test fluid, however, the composition of CMC was found to change from one supplier to the next. In addition, the inability to match the composition of each CMC sample to viscosity data from literature posed a problem. Viscosity standard gels were also considered for validation, however, the quantity required was found to be too large and would be too expensive.

Final molasses

Broadfoot and Miller (1990) carried out extensive research on the viscosity of molasses and massecuite using both a pipeline viscometer and a Brookfield RVT rotational viscometer. Broadfoot and Miller (1990) recommended that viscosity investigations be carried out within the range of shear rates of interest in order to minimise errors. The pipeline viscometer used in this investigation comprised of water-jacketed tubes attached to the base of a reservoir tank. Broadfoot and Miller (1990) found no statistically significant difference between the consistencies achieved with the pipeline viscometer and with the Brookfield viscometer. They also found no statistically significant difference in the flow behaviour indices for small length to diameter ratios, but for higher length to diameter ratios, the pipeline viscometer was found to give a consistent elevated flow behaviour index of 0.05 units.

Based on the close correlation of the values for consistency and flow behaviour index for molasses from the two rheological methods employed by Broadfoot and Miller (1990), together with the inability to source a suitable test fluid in sufficient quantities, C-molasses was used as the validation test fluid. Validation of the pipeline viscometer was conducted by comparison with independent viscosity analyses carried out by the Sugar Milling Research Institute NPC (SMRI) over the same range of shear rates. Experiments were conducted at 30 ^{0}C, allowing the viscosity parameters from the pipeline viscometer to be comparable with that of the Brookfield viscometer. T-type spindles were used.

Comparison of results

The pipeline viscometer was found to correlate well with the Brookfield viscometer for molasses measurements, with good agreement for the flow behaviour index, n. The consistency K for the pipeline viscometer was found to lie between 95 – 105 % of the Brookfield viscometer figures as seen in Table 3, with the exception of sample 1. The large discrepancy with results from sample 1 can be attributed to the low brix sample that proved difficult to handle.

Table 3. Comparison of results between viscometers for molasses viscosity

		N			K, Pa.s^n		
Sample number	Sample name	Brookfield viscometer	Pipeline viscometer	n Pipeline as % of Brookfield	Brookfield viscometer	Pipeline viscometer	K Pipeline as % of Brookfield
1	20161108am	0.74	0.75	102%	2.72	4.75	175%
2	20161108pm	0.83	0.83	100%	10.65	9.82	92%
3	20161109am	0.77	0.77	100%	18.92	17.90	95%
4	20161109pm	0.78	0.80	102%	12.37	12.97	105%
5	20161110	0.79	0.78	100%	31.98	29.56	92%

Massecuite Viscosity Results and Discussion

Repeatability tests

Nine massecuite samples were tested using the pipeline viscometer, each at six temperature intervals. No repeatability tests were carried out for the first three massecuite samples, however, the subsequent six samples were tested with repeats with respect to temperature as shown in Figures 10 to 15. Experiments were first carried out at increasing temperatures (blue markers), then decreasing temperatures (green markers) and once again at increasing temperatures (red markers), with the aim to achieve the same temperature set points along each trajectory.

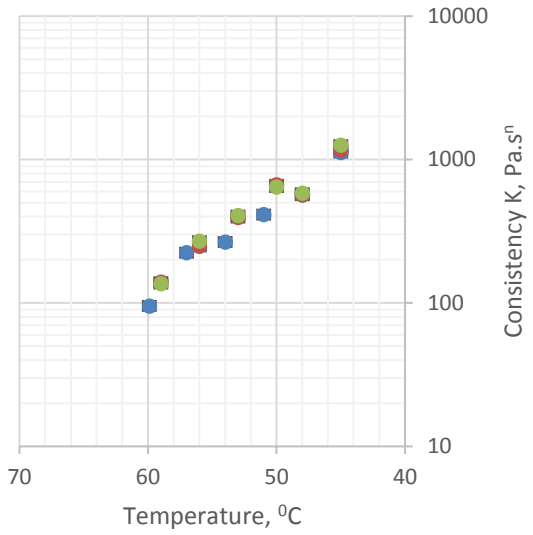

Figure 10. Sample 20160919

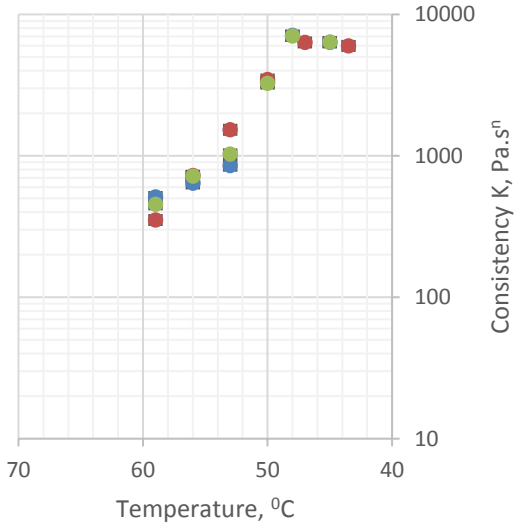

Figure 11. Sample 20160926

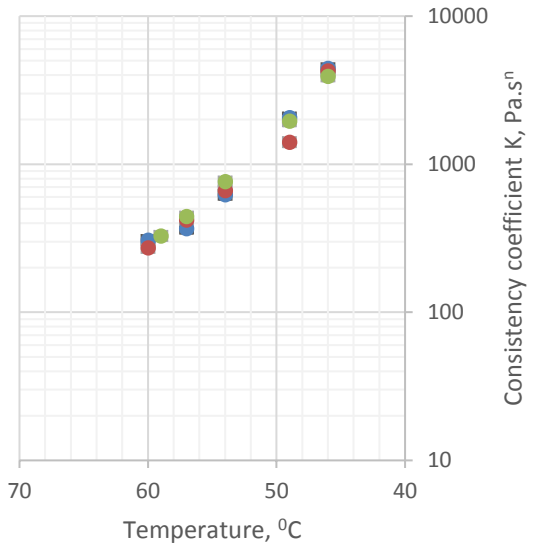

Figure 12. Sample 20161003

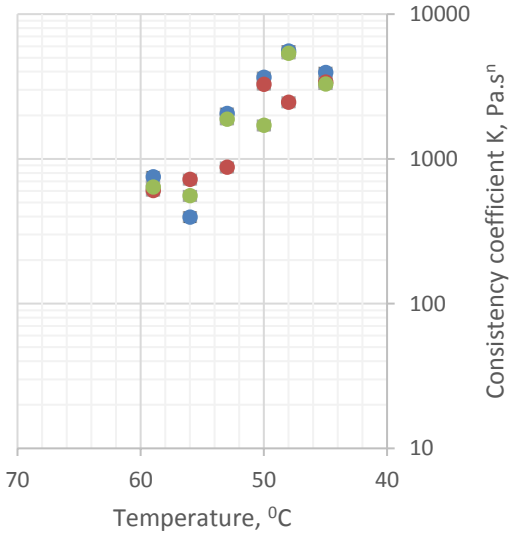

Figure 13. Sample 20161017

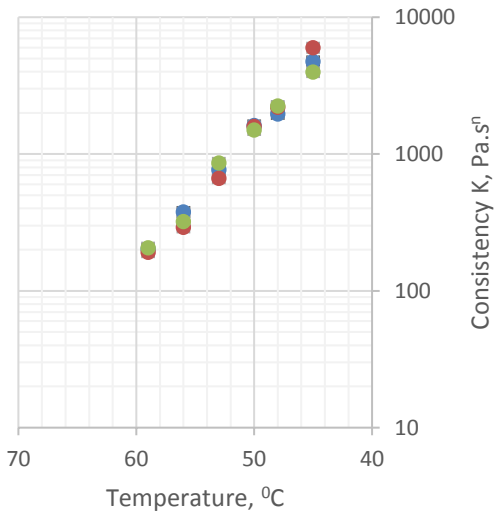

Figure 12. Sample 20161024

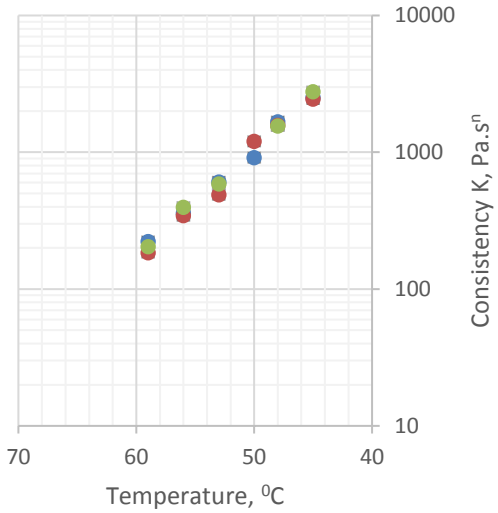

Figure 13. Sample 20161031

Slight fluctuations in air pressure of up to 2 kPa were noted whilst testing sample 20161017, contributing towards poor repeatability, as seen in Figure 13. The source of fluctuations was attributed to fluctuations in the main header pressure resulting in constant manual pressure regulation in order to achieve a constant pressure.

Care was taken to ensure massecuite temperatures remained constant for the duration of the experimental run, however, massecuite temperature fluctuations of up to 0.5 ^{0}C were noted as a result of thermal inertia. The massecuite temperature increased slightly at first, followed by a sharp rise in temperature. A similar trend was evident during cooling of massecuite. The temperature set point of the water bath was adjusted manually and required careful attention once the desired massecuite temperature was achieved to prevent temperature drift.

Flow behaviour index, n

The flow behaviour indices for all massecuite samples ranged between 0.8 and 0.9 and were not seen to fluctuate with temperature, as seen in Figure 16, and did not follow a trend with other properties of massecuite. This range is consistent with those reported by Awang and White (1976), and Barker (2008). The average flow behaviour index was found to be 0.85.

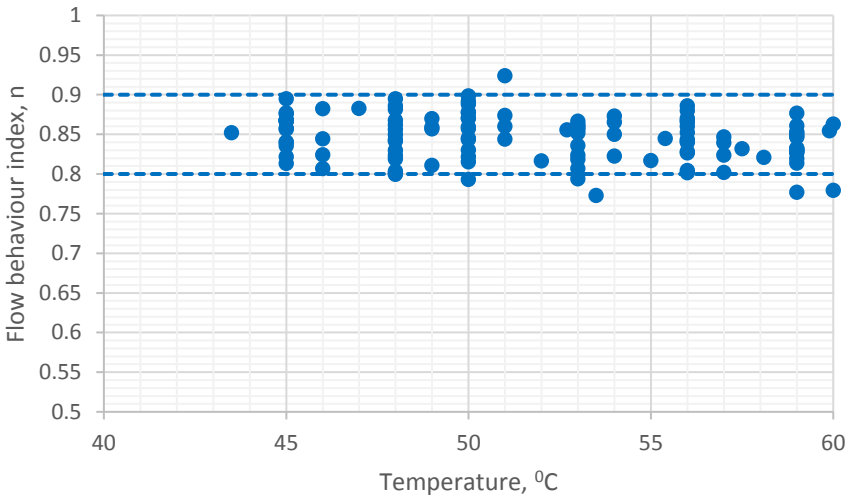

Figure 14. Flow behaviour index

Development of correlation for apparent viscosity of massecuite

In order to predict the apparent viscosity of massecuite, an average flow behaviour index of 0.85 can be used. The calculation of consistency, however, is somewhat more complex. A linear relationship between lnK and lnT was evident with an average slope of approximately -10.5 units.

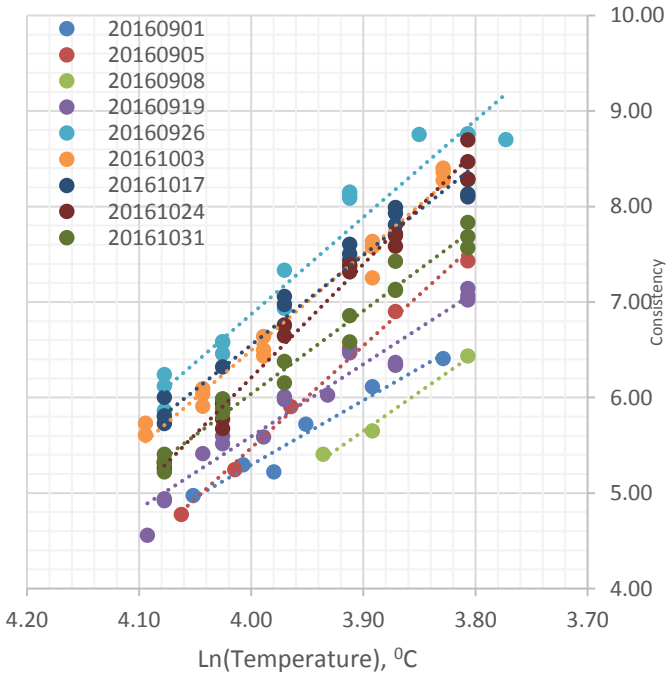

Figure 15. Relationship between consistency and temperature

The massecuite consistency was seen to increase with an increase in dry solids and crystal content and decrease with an increase in temperature. In addition to including the linear relationship between lnK and lnT, a coefficient for each variable was assumed and the square of the difference between the experimental and correlated consistencies was calculated and summed. The solver function was used to minimise the sum of the squared errors by optimising the coefficients associated with each variable. The coefficients for massecuite purity and dextran were found to be zero and the following correlation was proposed with a regression coefficient of 0.7672.

$$\ln K = \left(-10.5 \ln T + \frac{DS}{1.892}\right)\left(\frac{CC + 36}{100}\right) \qquad 21$$

The gradient of each line was found to be strongly dependent on temperature. The shift in the linear trend was found to be a strong function of crystal content and the intercept was found to be a function of massecuite dry solids.

A comparative plot of the correlation vs. experimental consistency is shown in Figure 18. Assuming a flow behaviour index of 0.85 and a shear rate of 1 s^{-1}, a comparative plot of correlation vs. experimental apparent viscosities is shown in Figure 19.

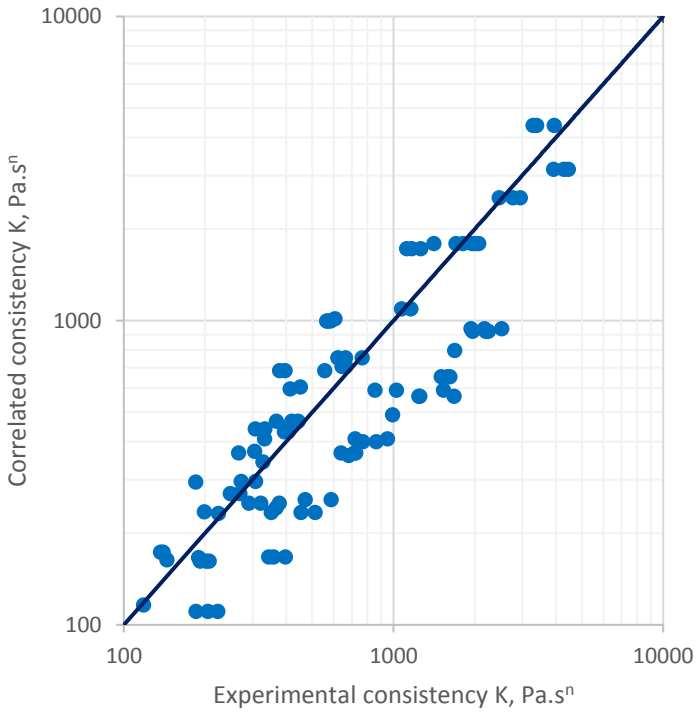

Figure 16. Comparison of experimental and calculated consistency

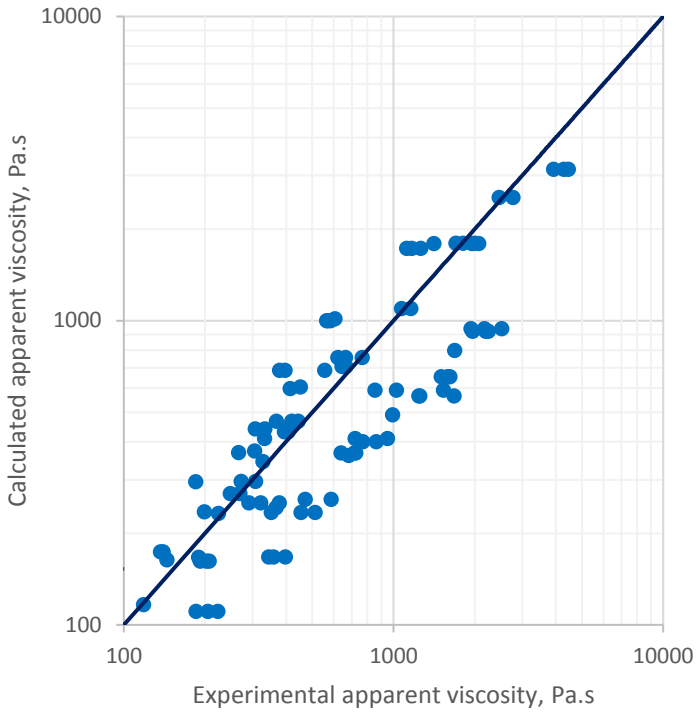

Figure 17. Comparison of experimental and calculated apparent viscosities (shear rate of 1 s^{-1})

No direct relationship was evident between consistency and massecuite purity or dextran. The dextran content ranged from 263 – 312 ppm on massecuite brix and the consistencies of some samples were elevated despite lower dextran levels and vice versa.

Comparison of experimental results with Rouillard (1984)
The viscosity data published by Rouillard (1984) assumed a dependence on temperature only and not on shear rate and is thus comparable to experimental results for a shear rate of $1s^{-1}$ i.e. when massecuite consistency is equal to massecuite viscosity.

Assuming a shear rate of $1s^{-1}$, the consistency for each experimental data point was superimposed on the range of viscosity recommended for C-massecuite by Rouillard (1984), as shown in Figure 20. A strong correlation between massecuite consistency and temperature was confirmed.

The upper limit and lower limit of C-massecuite viscosities, as recommended by Rouillard, (1984) are shown as solid bold lines in Figure 20 and can be represented by equations 22 and 23 respectively.

$$\mu_{upper\lim it} = 99991e^{-0.077T} \quad 22$$

$$\mu_{lower\lim it} = 15001e^{-0.077T} \quad 23$$

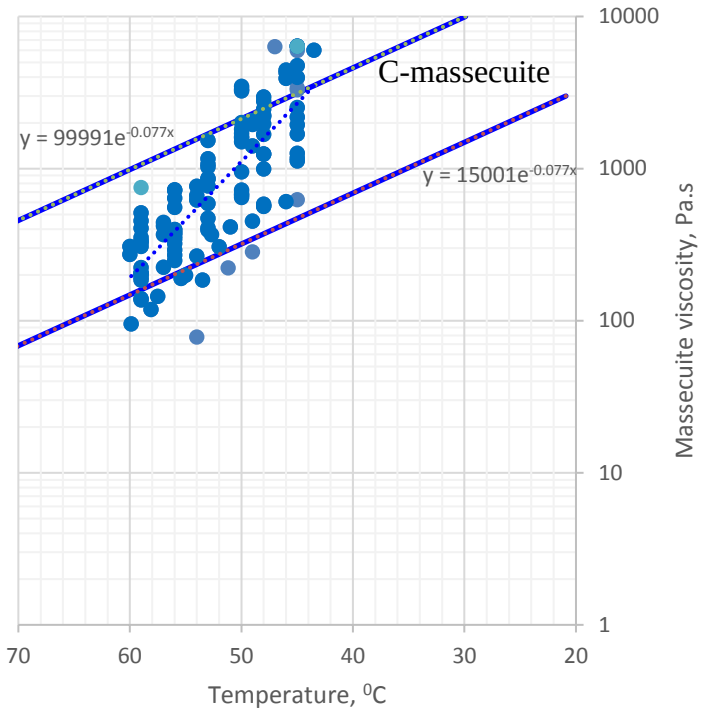

Figure 18. Experimental results compared to published range from Rouillard (1984) (shear rate of 1 s^{-1})

The current practice is for the upper-limit to be determined graphically from the viscosity chart developed by Rouillard (1984) at the desired temperature and for a sensible estimate of the C-massecuite viscosity to be carried out. The experimental data was found to fit within the band of values as represented by Rouillard (1984), confirming that the band currently used is appropriate, however, the rate of increase in viscosity with decreasing temperature was found to be greater than the prediction from Rouillard (1984).

Based on the experimental results, a new upper limit and a new lower limit of C-massecuite viscosities can be used, as shown by the dotted lines in Figure 21.

The new upper limit and new lower limit for C-massecuite viscosity can be calculated using equations 24 and 25 respectively in conjunction with the proposed correlation shown in equation 21, allowing a reasonable estimate for C-massecuite viscosity to be made. In order to apply the upper and lower limit equations to various shear rates, the proposed equations (24 and 25) are thus presented in terms of consistency rather than viscosity.

$$K_{upper\lim it} = 6\ 049136e^{-0.15T} \quad 24$$

$$K_{lower\lim it} = 765\ 243e^{-0.15T} \quad 25$$

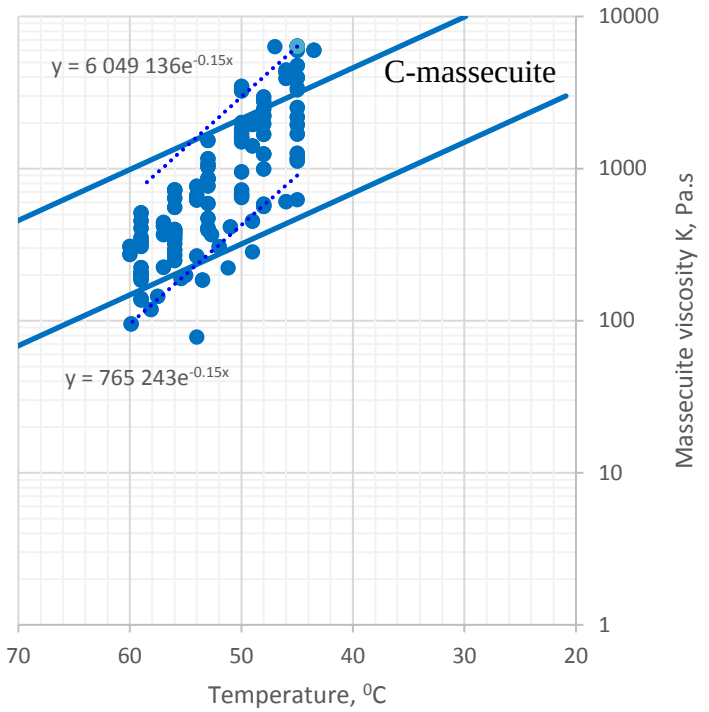

Figure 19. New proposed upper and lower limits for C-massecuite viscosity (shear rate of 1 s^{-1})

Conclusion

Despite a wide range of correlations and viscosity charts available for the determination of C-massecuite viscosity, most correlations were developed using data from rotating viscometry and thus possess an inherent uncertainty due to the interaction and displacement of crystals around the rotating spindle. The pipeline viscometer has been shown to be a reliable method of viscometry. However, few correlations were developed using this method of viscometry.

The correlation proposed by Ness (1980) does not take into account the effects of temperature and the correlation proposed by Bruhns (2004) is dependent on the accuracy of the molasses viscosity correlation utilised. In order to improve upon the estimation of C-massecuite viscosity, a pipeline viscometer was designed, constructed and validated using final molasses measurements from a rotating Brookfield viscometer.

The flow behaviour index for C-massecuite was found to lie between 0.8 and 0.9, with an average value of 0.85. A correlation was proposed for massecuite consistency as a function of temperature, dry substance and crystal content with a regression co-efficient of 0.7672. Although no direct relationship was evident between consistency and massecuite purity or dextran, there is a large amount of scatter in the comparison of correlated and experimental consistencies, suggesting that massecuite viscosity remains a function of impurities not taken into account during analyses.

Assuming a shear rate of $1s^{-1}$, the experimental data was found to fit within the range of C-massecuite values recommended by Rouillard (1984), as shown in Figure 20, confirming that the band currently used in Figure 3 is appropriate. However, the rate of increase in viscosity with decreasing temperature was found to be greater than the prediction from Rouillard (1984). Based on the experimental results in conjunction with the viscosity chart proposed by Rouillard (1984), a new upper limit and a new lower limit for C-massecuite consistency was proposed, as shown by the dotted lines in Figure 21 and expressed according to equations 24 and 25

respectively. These equations can be used together with the proposed correlation shown in equation 21 to ensure a reasonable estimate for C-massecuite viscosity can be made.

Acknowledgements

I would like to thank Dr David Lokhat, Steve Peacock, Chandresh Narotam, Patrick Moodley and the team at Tongaat Hulett's Maidstone mill for their unreserved support and assistance with the construction of the pipeline viscometer. I'd also like to thank Sibonelo Goodman Mchunu and Sphakamiso Zondi for their cheerful approach and dedicated assistance with experimental work.

Nomenclature

Greek Symbols

Δh = Hydrostatic head, m
ΔP_e = Pressure drop due to entrance effects, kPa
ΔP_c = Corrected pressure drop due to entrance effects, kPa
ΔP = Pressure drop, kPa
ϕ = Volume fraction of crystal
ϕ_m = Maximum volume fraction of crystals
γ = Shear rate, s^{-1}
μ = Viscosity, Pa.s
ρ = Density, kg/m^3
σ_j = Deviation associated with variable j
τ = Shear stress, Pa
τ_w = Shear stress at the pipe wall, Pa

Variables

B = Massecuite brix, %
CC = Crystal content, %
CV = Coefficient of variation
D = Pipe diameter, m
DS = Dry substance, %
g = Acceleration due to gravity, $9.81 m/s^2$
K = Consistency, $Pa.s^n$
l = Mean crystal size by mass (as determined by sieve analysis), mm
l_{sgs} = Specific grain size or mean crystal size by area, mm
L = Pipe length, m
L_{eff} = Effective length, m
l_{sgs} = Specific grain size or mean crystal size by area, mm
n = Flow behaviour index
N = Speed, rpm
NS = Non-sucrose, %
P = Pressure, kPa
P = Purity, %
Q = Volumetric flow, m^3/s
Q_{ns} = Non-slip volumetric flow, m^3/s
Q_s = Volumetric flow due to wall slip, m^3/s

R = Pipe radius, m
Re = Reynold's number
R_s = Radius of spindle, m
RS/Ash = Reducing sugar to ash ratio
S/NS = Sucrose to Non-sucrose ratio
SS_E = Error sum of squares
SS_R = Residual sum of squares
SS_T = Total sum of squares
T = Temperature, ^{0}C (unless otherwise stated)
t = Torque, N.m
TS = Total solids, %
u = Fluid velocity, m/s
u_c = Corrected fluid velocity, m/s
u_{ns} = Non-slip fluid velocity, m/s
u_s = Wall slip fluid velocity, m/s
x_j = Measured statistical value for variable j
X = Volume fraction of liquid phase
z = Height, m

REFERENCES

Adkins BG (1951). Notes on the viscosity of molasses and massecuite. *Proc. Qd. Soc. Sugar Cane Technol.,* Volume 18, pp. 43-52.

Ananta T, Delavier HJ, Kamarijani and Mugiono (1989). The applicability of rotational viscometers to measure rheological properties of massecuites. *Proc. Int. Soc. Sugar Cane Technol.,* Volume 20, pp. 78-88.

Artyukhov YG and Garyazha VT (1970). Rheology of massecuites. *Izvest. VUZ. Pisch Tekhnol.,* Volume 4, pp. 157-162.metz

Awang M and White ET (1976). Effect of crystal on the viscosity of massecuites. *Proc. Qd. Soc. Sugar Cane Technol.,* Volume 43, pp. 263-270.

Barker B (1998). Theoretical and practical considerations on the rheology of sugar products. *Proc. S. Afr. Sugar Technol. Ass.,* Volume 72, pp. 300-305.

Barker B (2008). Massecuite consistency measurement using a pipeline viscometer. *Proc. S. Afr. Sugar Technol. Ass.,* Volume 81, pp. 227-233.

Behne MF (1964). Viscometry in massecuites. *Proc. Qd. Soc. Sugar Cane Technol.,* Volume 31, pp. 289-296.

Broadfoot R (1984). Viscosity limitations on massecuite exhaustion. *Proc. Aust. Soc. Sugar Cane Technol.,* Volume 6, pp. 279-286.

Broadfoot R and Miller KF (1990). Rheological studies of massecuites and molasses. *International Sugar Journal,* 92(1098), pp. 107-146.

Broadfoot R, Miller KF and McLaughlin RL (1998). Rheology of high grade massecuites. *Proc. Aust. Soc. Sugar Cane Technol.,* Volume 20, pp. 388-397.

Bruhns M (2004). The viscosity of massecuite and its suitability for centrifuging. *Zuckerindustrie Journal,* 29(12), pp. 853-863.

Chhabra RP and Richardson JF (2008). *Non-Newtonian flow and applied rheology.* 2nd ed. Oxford: Butterworth-Heinemann.

Durgueil EJ (1987). Determination of the consistency of non-Newtonian fluids using a Brookfield HBT viscometer. *Proc. S. Afr. Sugar Technol. Ass.,* Volume 61, pp. 32-39.

Echeverri LF, Rein PW and Acharya S (2005). Numerical and experimental study of the flow in vacuum pans. *Int. Soc. Sugar Cane Technol.,* Volume 25, pp. 212-228.

Holland FA and Bragg R (1995). *Fluid flow for Chemical Engineers.* Oxford: Butterworth Heinemann.

Keast WJ and Sichter NJ (1984). Vertical continuous crystallizer - Victoria mill. *Proc. Aust. Soc. Sugar Cane Technol.,* Volume 6, pp. 293-299.

Kelly FHC and McAntee H (1942). The viscosity of molasses and massecuite. *Proc. Qld. Soc. Sugar Cane Technol.,* Volume 13, p. 51.

Kelly FHC (1958). Viscosity of crystal suspensions. *Sharkara,* Volume 1, pp. 37-45.

Kot YD, Yasinshaya TV and Sushenko AK (1968). Viscous properties of massecuites. *Sakh. Prom.,* pp. 106-125.

Love DJ (2002). Estimating dry solids and true purity from brix and apparent purity. *Proc. S. Afr. Sugar Technol. Ass.,* Volume 76, pp. 526-532.

Metzler E (1996). *Rheology of suspensions at high solids concentrations.* Brisbane: Thesis for bachelor of engineering, The University of Queensland.

Mueller S, Llewellin EW and Mader HM (2011). The effect of particle shape on suspension viscosity and implications for magmatic flows. *Geophysical Research Letters,* 38(13).

Ness JN (1980). Massecuite viscosity - some observations with a pipeline viscometer. *Proc. Aust. Soc. Sugar Cane Technol.,* Volume 2, pp. 195-200.

Ness JN (1983). On the measurement of massecuite flow properties. *Proc. Aust. Soc. Sugar Cane Technol.,* Volume 18, pp. 1295-1303.

Perry JH (1950). *Chemical Engineers' Handbook.* 3rd ed. New York: McGraw-Hill.

Rein P (2007). *Cane Sugar Engineering.* Berlin: Verlag Dr Albert Bartens KG.

Rouillard EEA (1984). *Viscosity of factory products,* Durban: Sugar Milling Research Institute Technical report no. 1375, pp. 1-16

Rouillard EEA (1985). *The study of boiling parameters under conditions of laminar non-Newtonian flow with particular reference to massecuite boiling.* Durban: PhD thesis, University of Natal.

Rouillard EEA and Koenig MFS (1980). The viscosity of molasses and massecuite. *Proc. S. Afr. Sugar Technol. Ass.,*Volume 54, pp. 89-92.

Seeton CJ (2006). Viscosity - temperature correlation for liquids. *Tribology Letters,* 22(1), pp. 67-78.

Silina N (1953). Viscosity of massecuite. *Sakhar. Prom.,* Volume 8, pp. 4-10.